The Abdus Salam International Centre for Theoretical Physics

United Nations Educational, Scientific and Cultural Organization

IAEA
International Atomic Energy Agency

1856-24

2007 Summer College on Plasma Physics

30 July - 24 August, 2007

Electromagnetic radiation generation by relativistic electron beams

A. Phelps

SUPA, Physics Department
University of Strathclyde
Glasgow, Scotland, U.K.

Electromagnetic radiation generation

by

relativistic electron beams

Alan Phelps

SUPA, Physics Department, University of Strathclyde,

Glasgow, Scotland, UK

Intense Energetic Electron Beams

Interacting with Electromagnetic Fields

Electromagnetism - Maxwell

Collective - Plasma Effects

Non-linearity

Special Relativity

Basic equations

$$\frac{d\underline{p}}{dt} = e\left(\underline{E} + \underline{v} \times \underline{B}\right) \qquad \underline{p} = \gamma m_0 \underline{v} \qquad \gamma = \frac{1}{\sqrt{1 - \frac{v^2}{c^2}}}$$

γ in our experiments is typically between 1 and 2 ie mildly relativistic

$$\underline{\nabla} \cdot \underline{D} = \rho \qquad \underline{\nabla} \times \underline{E} = -\frac{\partial \underline{B}}{\partial t}$$

$$\underline{\nabla} \cdot \underline{B} = 0 \qquad \underline{\nabla} \times \underline{H} = \underline{j} + \frac{\partial \underline{D}}{\partial t}$$

Particle in Cell (PiC) Codes

A PiC code, time steps Maxwell's equations on a mesh.

On each time step it computes the motion of particles within each cell. Each particle within a cell will have a position and velocity. The current source terms in Maxwell's equations are derived by taking an average of all the particles in a cell. This average can be smoothed between cells to enhance stability and accuracy.

PiC codes can be 2D or 3D

For our simulations we use either MAGIC, KARAT, or SURETraj

Energy levels of electrons in a magnetic field

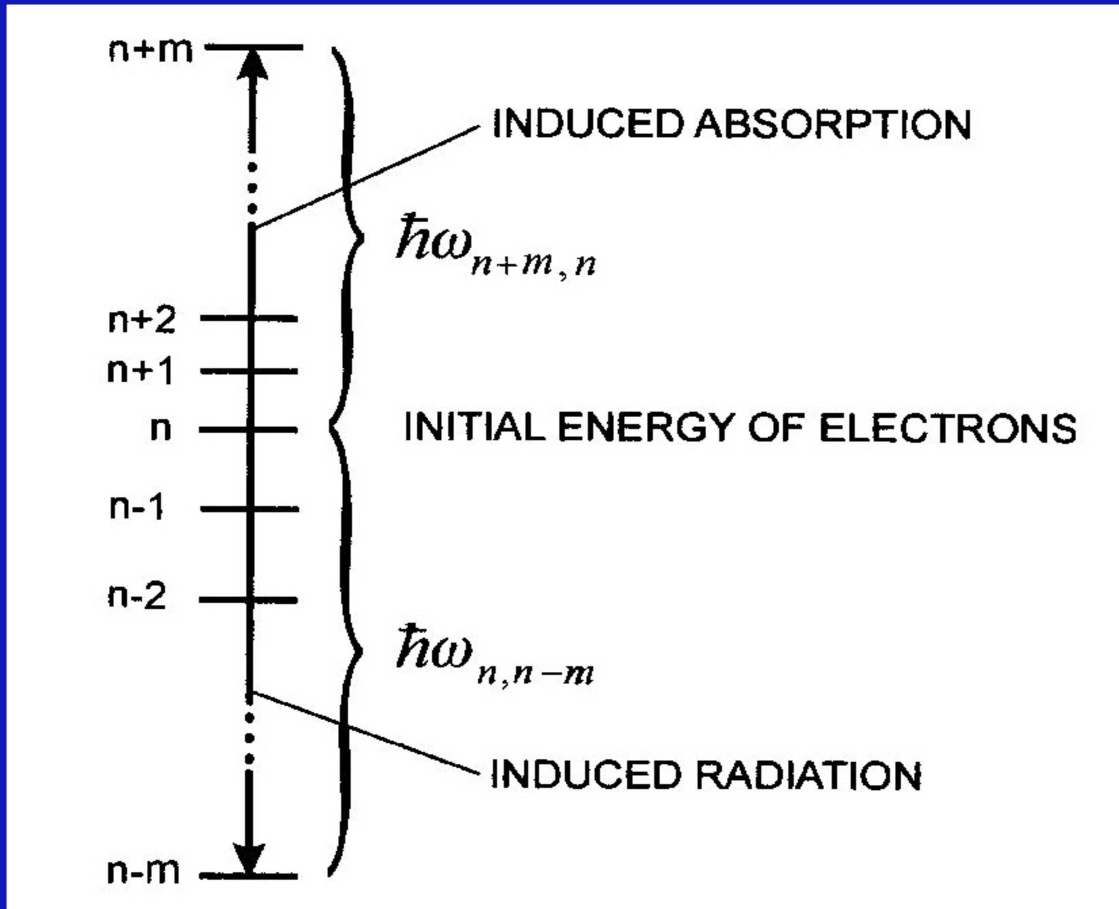

Asymmetrical gain curve at cyclotron resonance for relativistic electrons

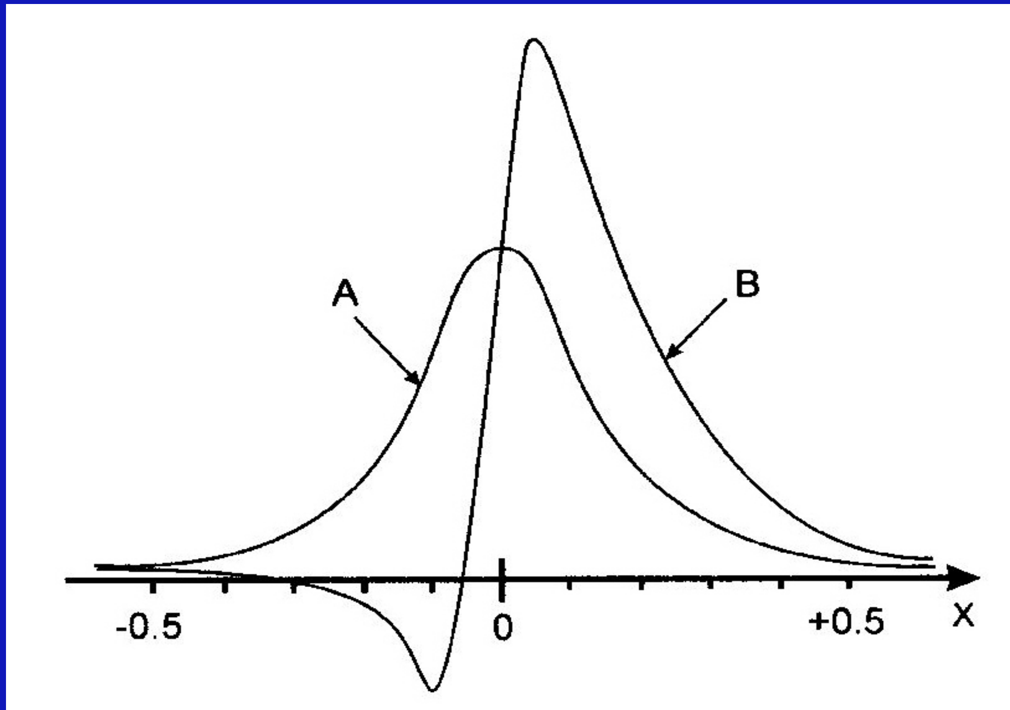

A – nonrelativistic
B - relativistic

Equations for electron beam mode and waveguide mode.

$$\omega = s\omega_c + k_z v_z$$

$$\omega^2 = \omega_{co}^2 + k_z^2 c^2$$

Where s is an integer, ω_c is the cyclotron frequency and ω_{c0} is the cut-off frequency of the waveguide.

where $\omega_c = \dfrac{eB}{\gamma m_0}$ $\qquad \gamma = (1 - \dfrac{v^2}{c^2})^{-1/2}$

Gyro-radiation sources

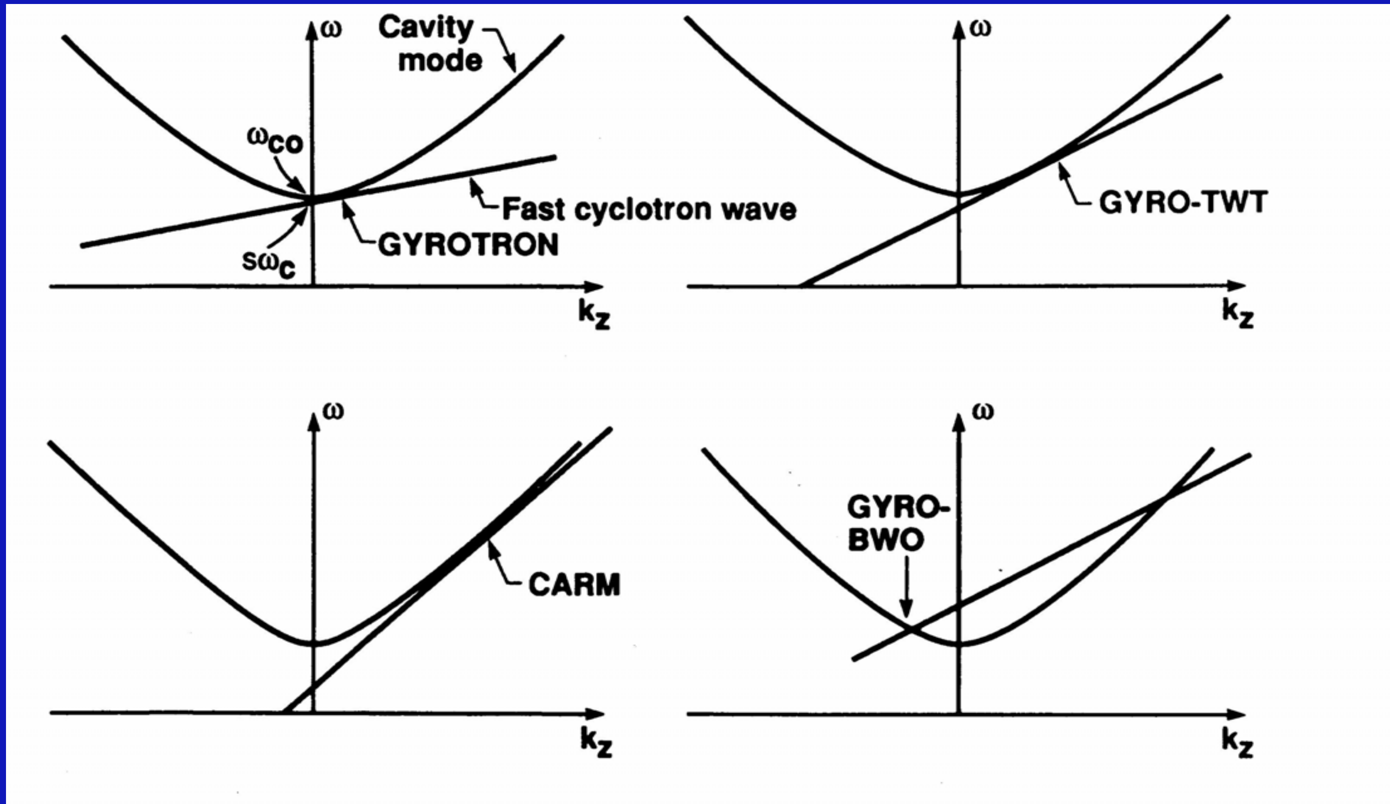

$$\omega = s\omega_c + k_z v_z$$

$$\omega^2 = \omega_{co}^2 + k_z^2 c^2$$

Electron Cyclotron Maser

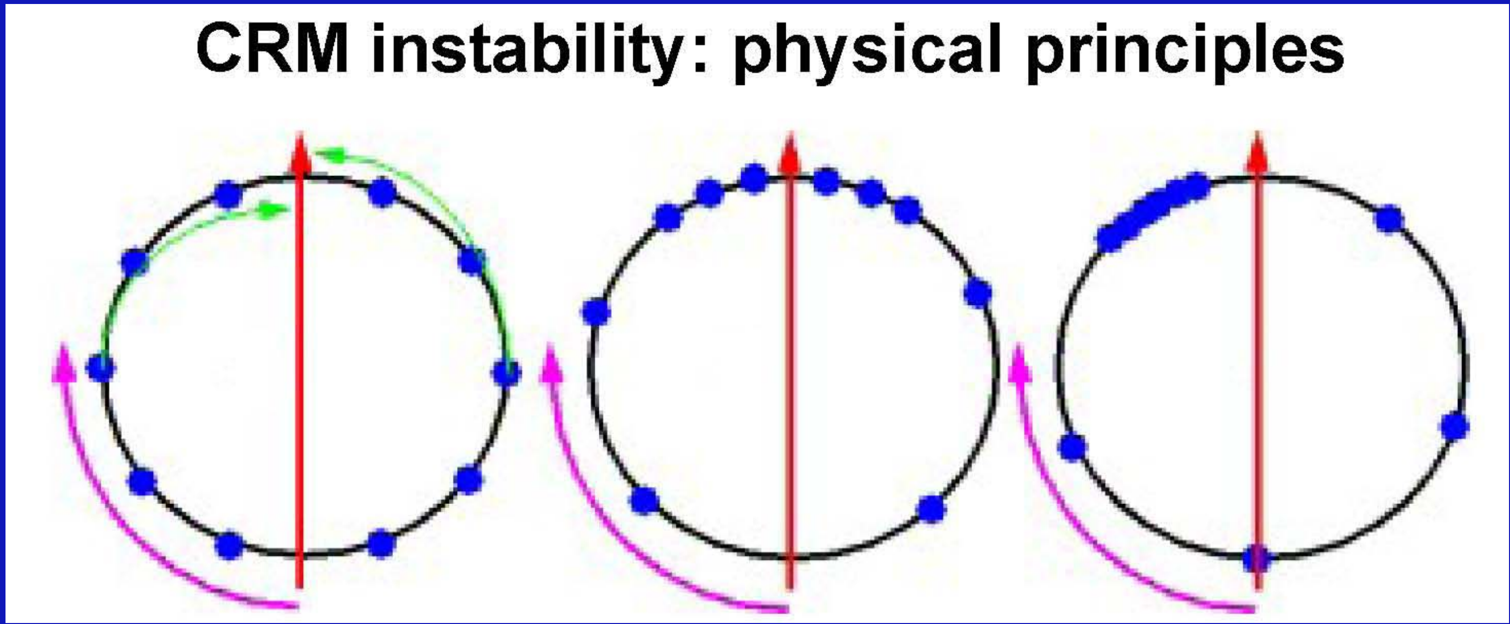

$$\omega_c = \frac{eB}{\gamma m_0}$$

- Electrons co-rotating with the transverse electric field of an electromagnetic radiation mode.
- Electrons subject to deceleration are advanced in phase by the relativistic dependence of the cyclotron frequency, those subject to acceleration are retarded in phase resulting in a bunch.

Gyrotron

Successful manifestation of the Electron Cyclotron Maser

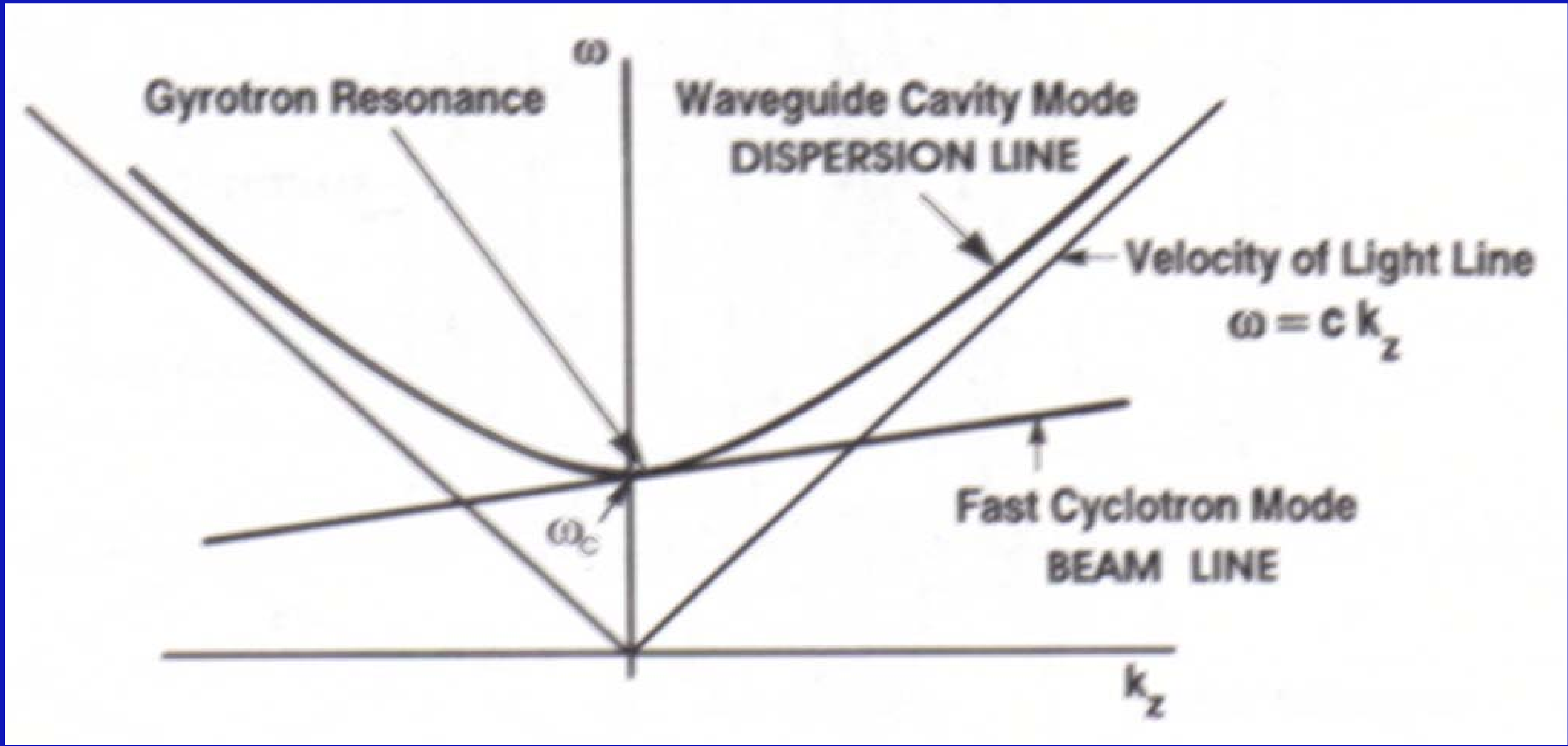

Garven M., Spark S.N., Cross A.W., Cooke S.J. and Phelps A.D.R., 1996, Phys. Rev. Lett., **77**, 2320-2323

Cooke S.J., Cross A.W., He W. and Phelps A.D.R., 1996, Phys. Rev. Lett., **77**, 4836-4839.

Harmonic gyrotron

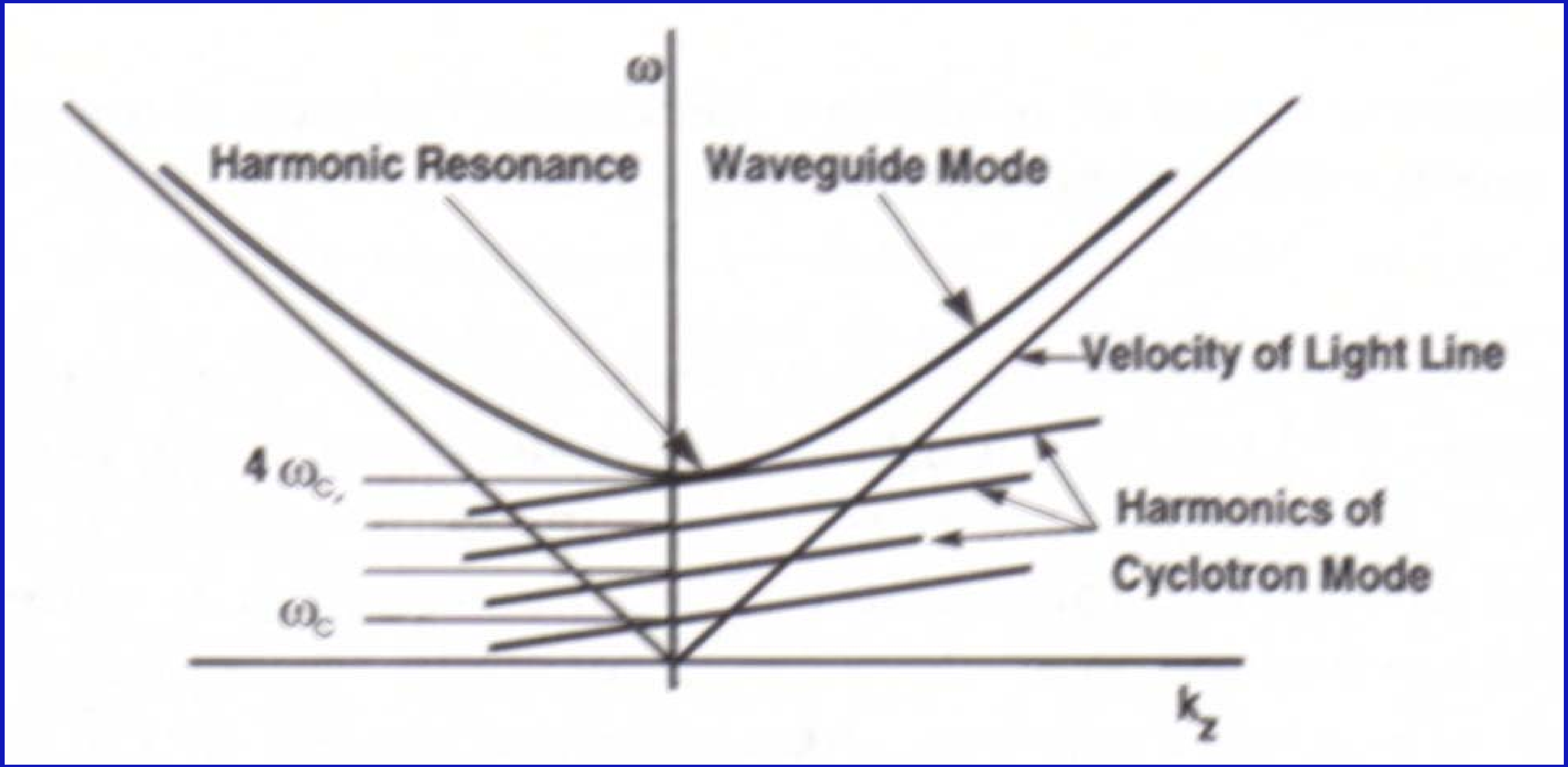

Schematic of a gyrotron

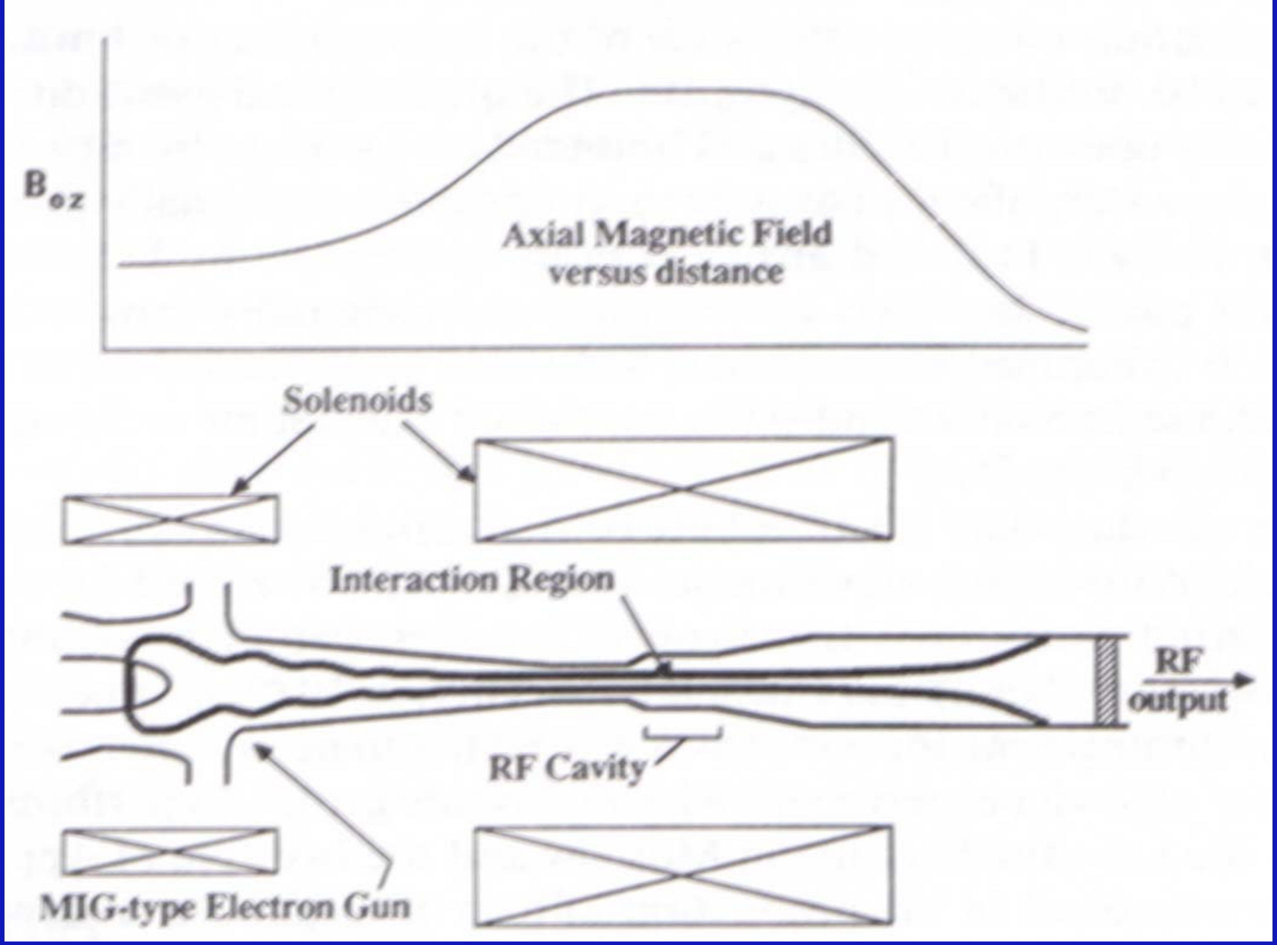

Gyro -TWA amplifier schematic.

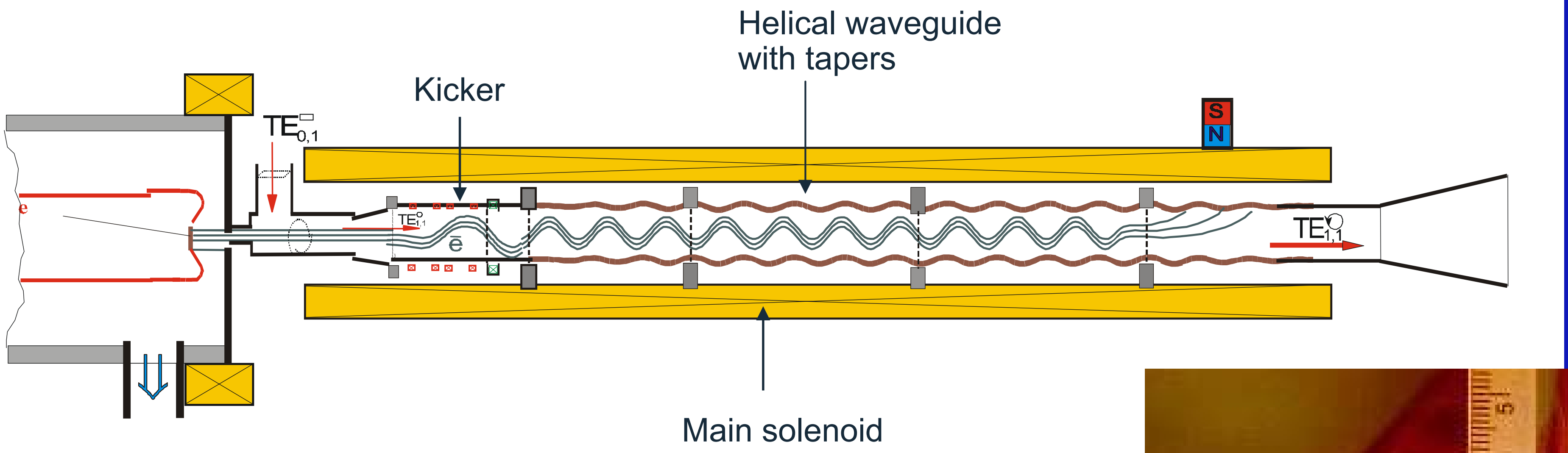

Measured Gyro-TWA Performance

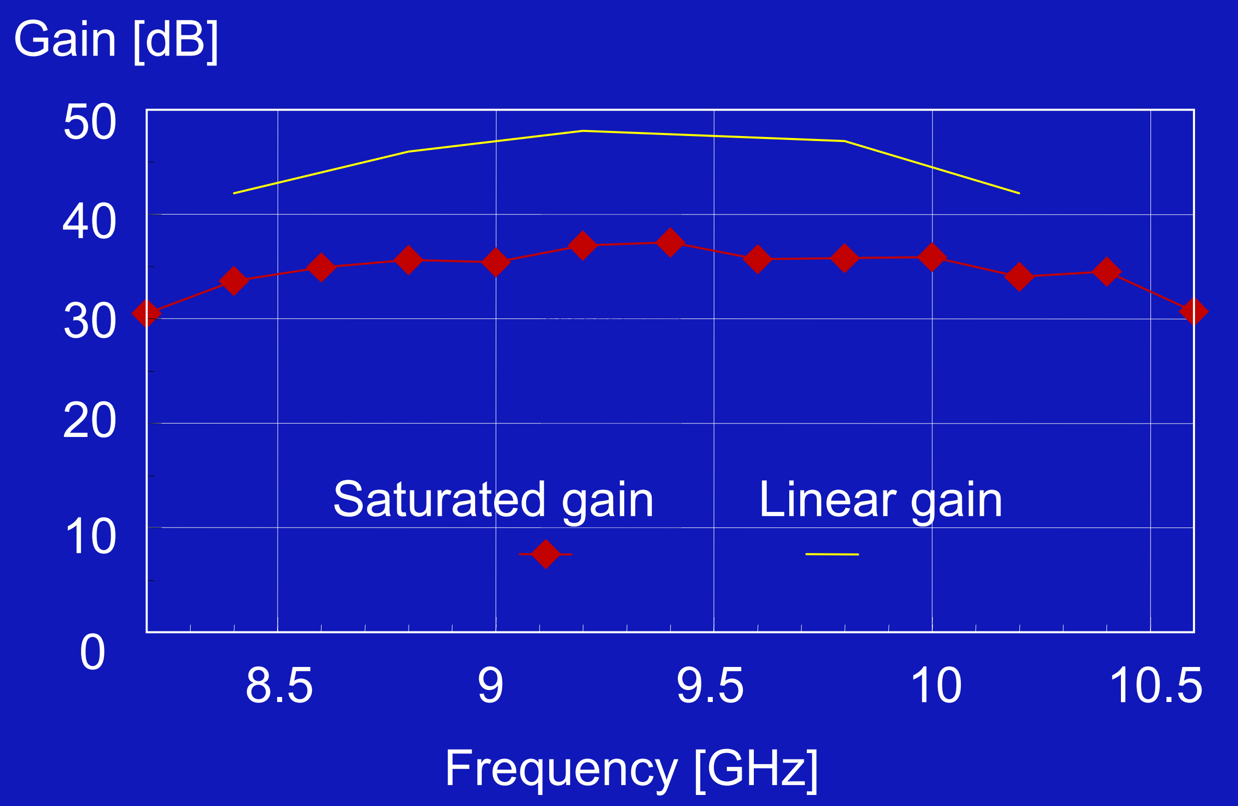

Gyro-TWA results

The helically corrugated interaction waveguide allows high power, high frequency, high efficiency, high gain, wide band interaction, whilst simultaneously mitigating the problem of absolute instabilities.

Strathclyde helical gyro-TWT achieved:

1.1MW output power (TE_{11}), 29% efficiency, 21% frequency bandwidth (3dB points) centred at 9.4GHz, Saturated gain 37dB, linear gain 48dB

Denisov G.G., Bratman V.L., Cross A.W, He W., Phelps A.D.R., Ronald K., Samsonov S.V. and Whyte C.G., 1998, Phys. Rev. Lett., **81**, 5680-5683

Bratman V.L., Cross A.W., Denisov G.G., He W., Phelps A.D.R., Ronald K., Samsonov S.V., Whyte C.G. and Young A.R., 2000, Phys. Rev. Lett., **84**, 2746-2749

Electromagnetic wave compression using a frequency chirp in a dispersive system

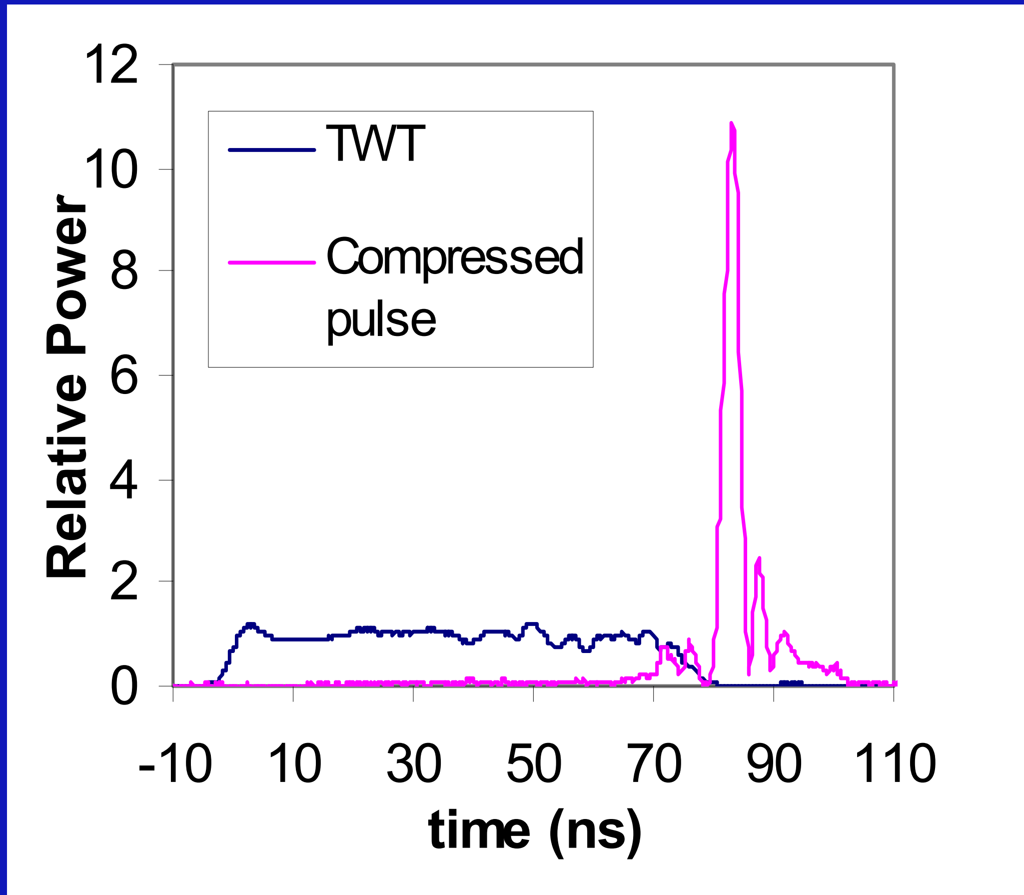

S.V. Samsonov, A.D.R. Phelps, V.L. Bratman, G. Burt, G.G. Denisov, A.W. Cross, K. Ronald, W. He and H. Yin, Phys. Rev. Lett., 2004, 92, 118301, 1-4.

Schematic of FEL

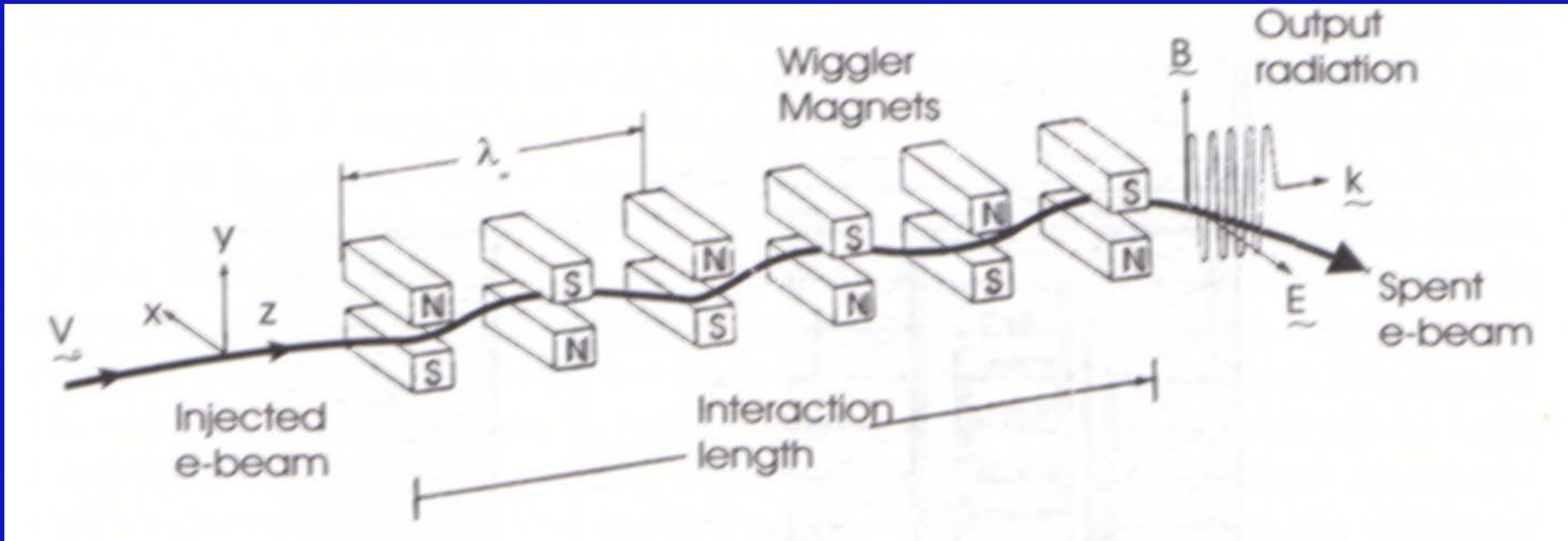

FEL fundamental formulae

The peak of the spontaneous emission spectrum from a magnetic undulator of wavelength λ_w for free relativistic electrons occurs at a wavelength λ given by

$$\lambda = \frac{\lambda_w (1 + K^2 / 2)}{2\gamma^2}$$

where $\gamma = \left(1 - \frac{v^2}{c^2}\right)^{-1/2}$ and $K = 93.4 \lambda_w B_w$

λ can range from microwave to X-ray wavelengths

FEL gain curve is asymmetric about resonance frequency

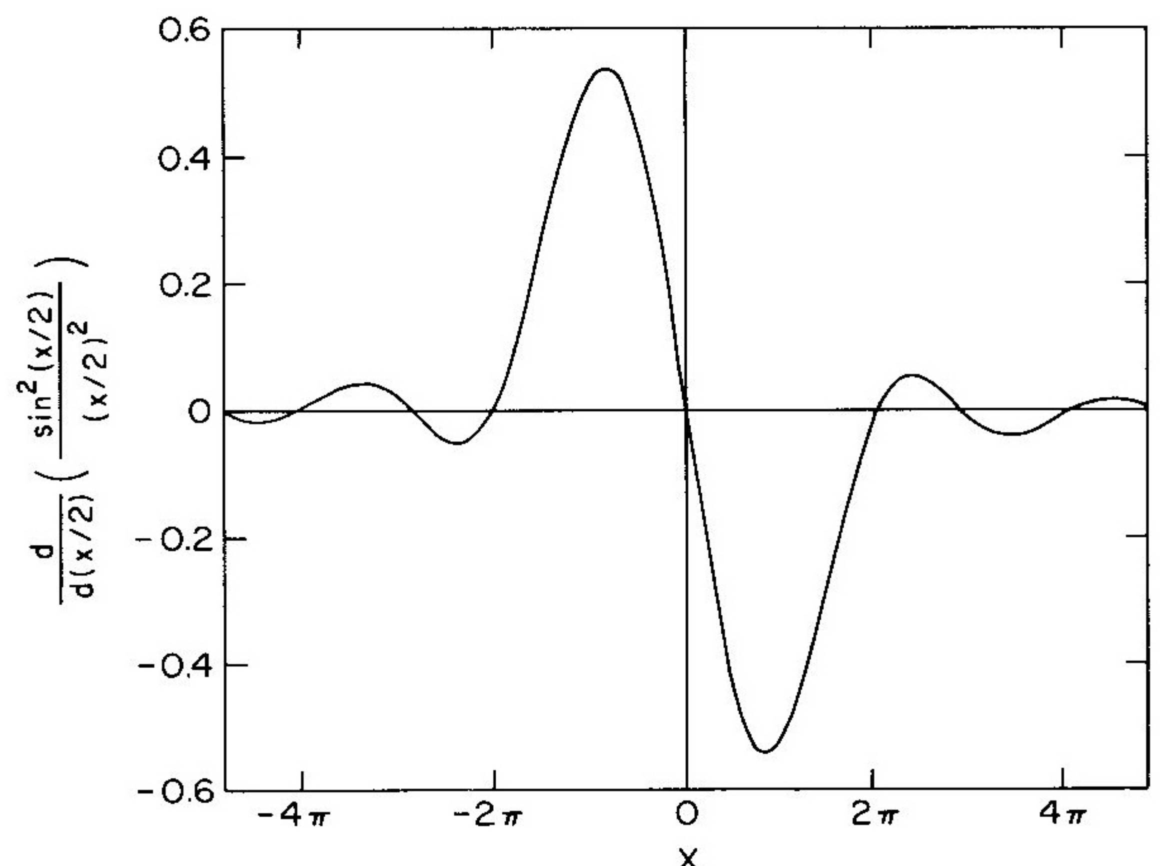

Ubitron
Undulated beam interaction electron tube

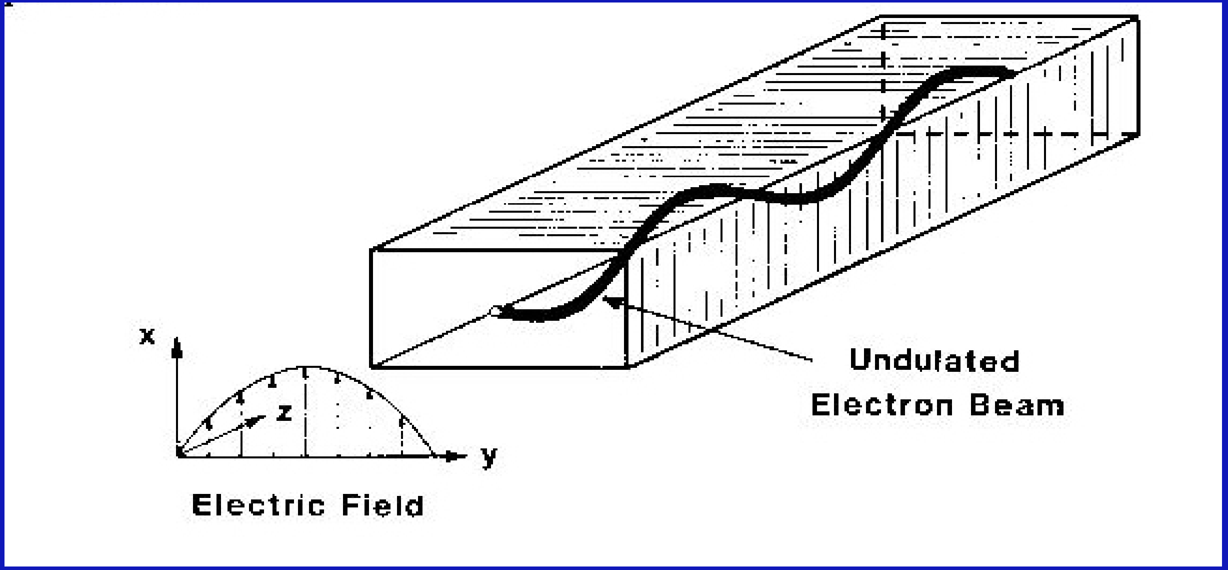

Ubitron

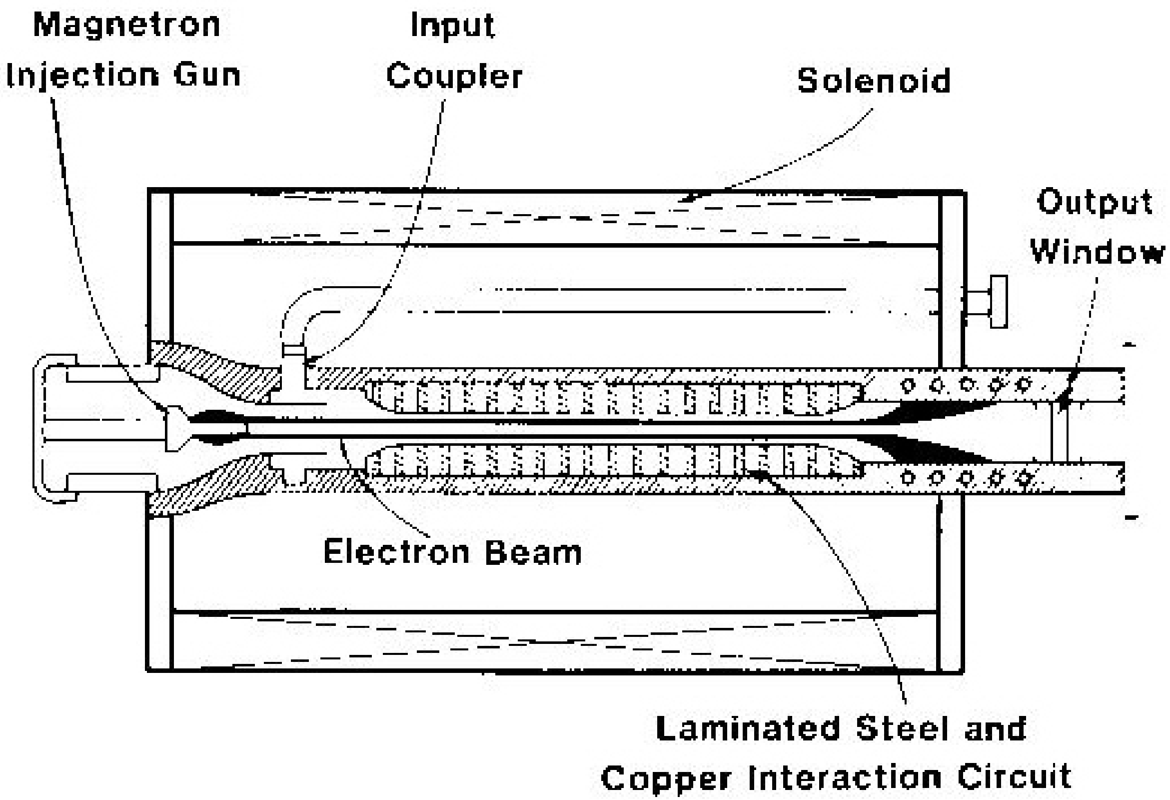
Magnetron
Injection Gun
Input
Coupler
Solenoid
Output
Window
Electron Beam
Laminated Steel and
Copper Interaction Circuit

2D Bragg HPM sources

Generic method to increase power limits from a few GW to 100GW in 100ns pulses

1 GW in a 100ns pulse provides a 100J pulse

100GW in a 100ns pulse provides a 10kJ pulse

These Free Electron Laser pulse energies compare favourably with the energy within a single pulse from present conventional lasers

Two Dimensional Bragg Design

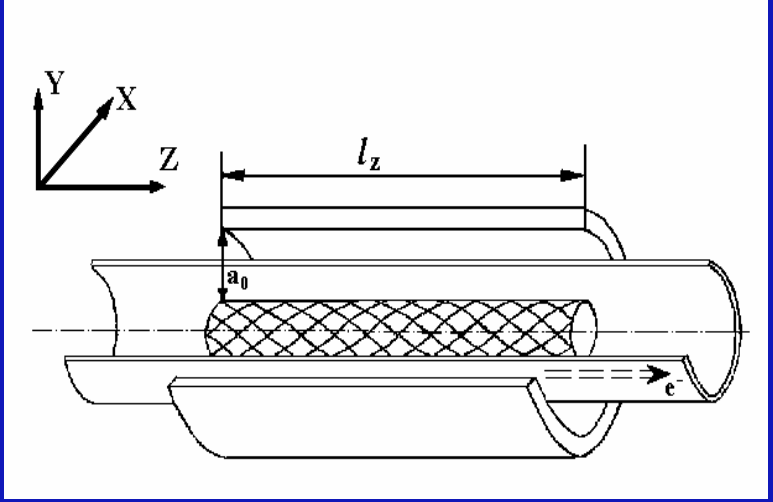

This surface where white squares indicate recesses and black squares indicate untouched parts of the waveguide wall can be described under the assumption $K_x = K_z$ as:

$$F(x,z) = \frac{4}{\pi}\left(\cos(K(x-z)) + \cos(K(x+z))\right)$$

The field scattering on the 2D Bragg structure taking into account the Bragg conditions can be described by the system of equations:

$$\pm\frac{\partial A_\pm}{\partial z} + i\delta A_\pm + i\alpha_2\left(B_+ + B_-\right) = 0$$

$$\pm\frac{\partial B_\pm}{\partial x} + i\delta B_\pm + i\alpha_2\left(A_+ + A_-\right) = 0$$

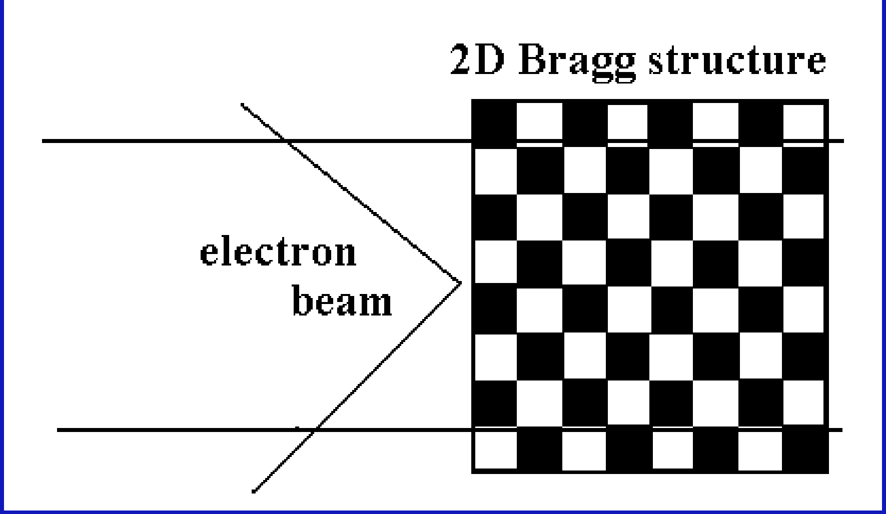

where α_2 is the coupling coefficient and δ is the detuning from the Bragg frequency.

1D and 2D Bragg Reflectors

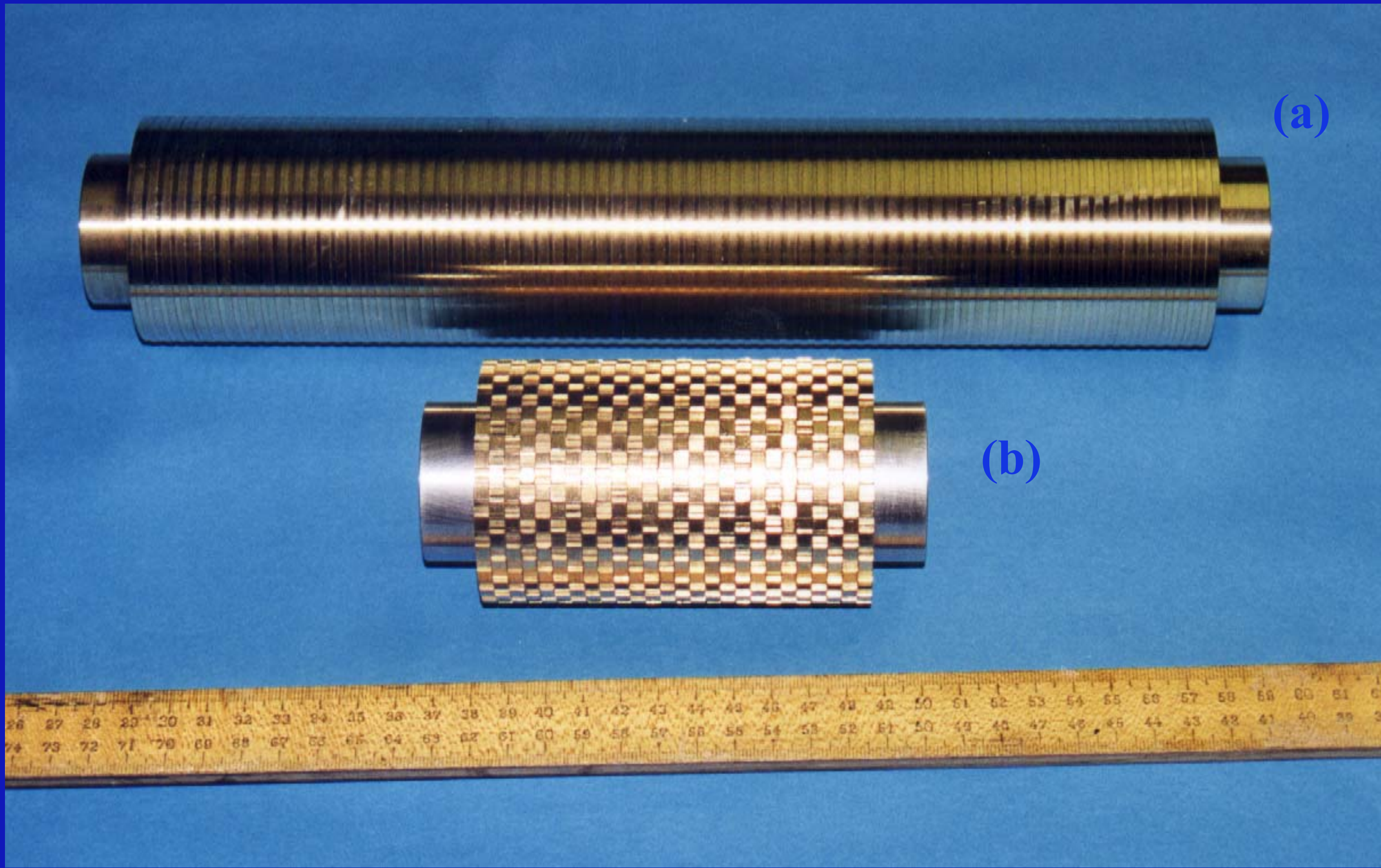

(a) the 1D Bragg reflector length 30cm (b) the 2D Bragg reflector length 10.4cm

The Strathclyde 2D Bragg Free Electron Laser

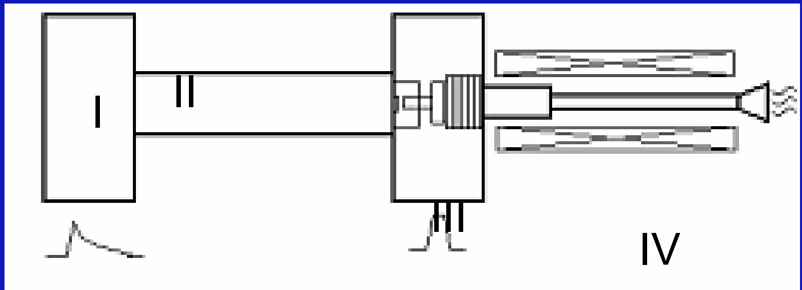

Schematic diagram of FEL experimental set-up: (I) Marx Pulsed Power (MPP) supply; (II) transmission line; (III) Spark gap & HCA; (IV) guide solenoid coaxial drift tube which includes the FEL interaction space

a)

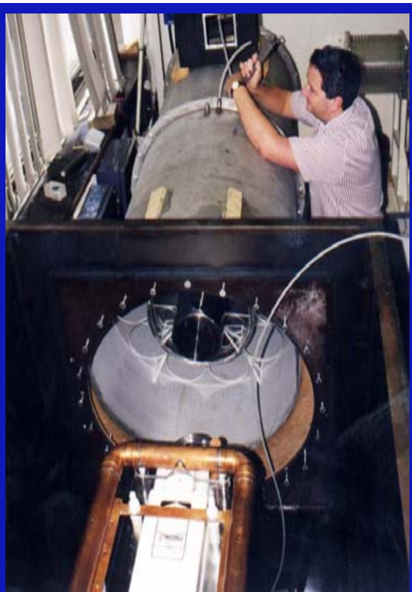

b)

c)

d)

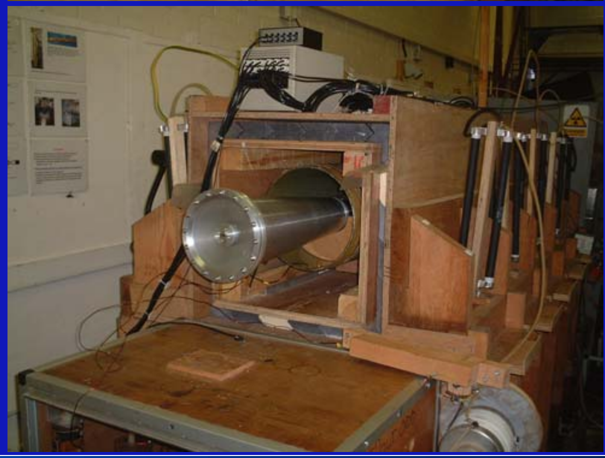

The photograph of the (a) MPP supply and the transmission line; (b) guide solenoid capacitors' support structure ; c) HCA with coaxial electron drift tube; (d) HCA fully assembled with guide solenoid, beam diagnostics and X-ray shielding

EM radiation output from 2D Bragg Free Electron Laser

Excitation of a neon light bulb panel due to generation of 60MW millimetre-wave electromagnetic radiation

I.V. Konoplev, P. McGrane, W. He, A. W. Cross, A. D. R. Phelps, C. G. Whyte, K. Ronald, and C. W. Robertson , Phys. Rev. Lett., **96**, 035002 (2006)

Superradiant Free Electron Sources

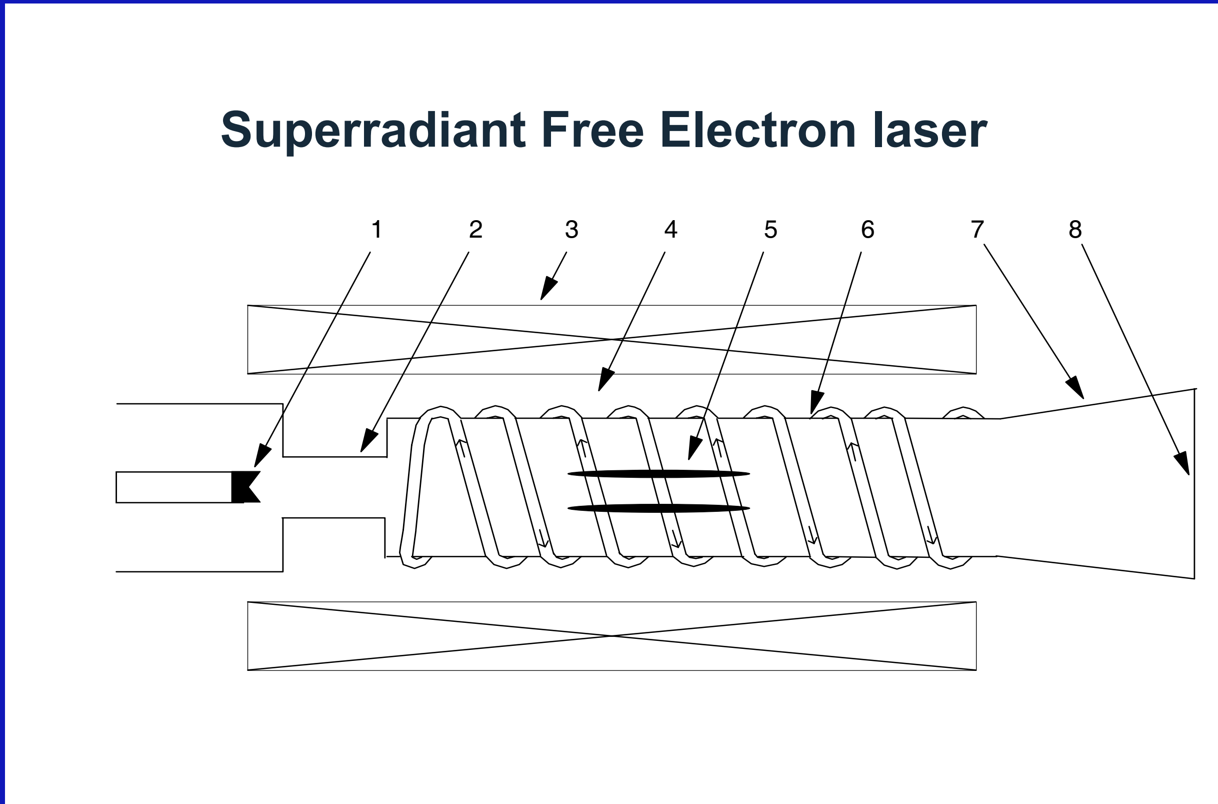

(1) cathode (2) cut-off (3) solenoid (4) wiggler (5) electron bunch
(6) waveguide (7) taper (8) window

Robb G.R.M., Ginzburg N.S., Phelps A.D.R. and Sergeev A.S.,

1996, Phys. Rev. Lett., <u>77</u>, 1492-1495.

Superradiant Free Electron Sources

Superradiant BWO

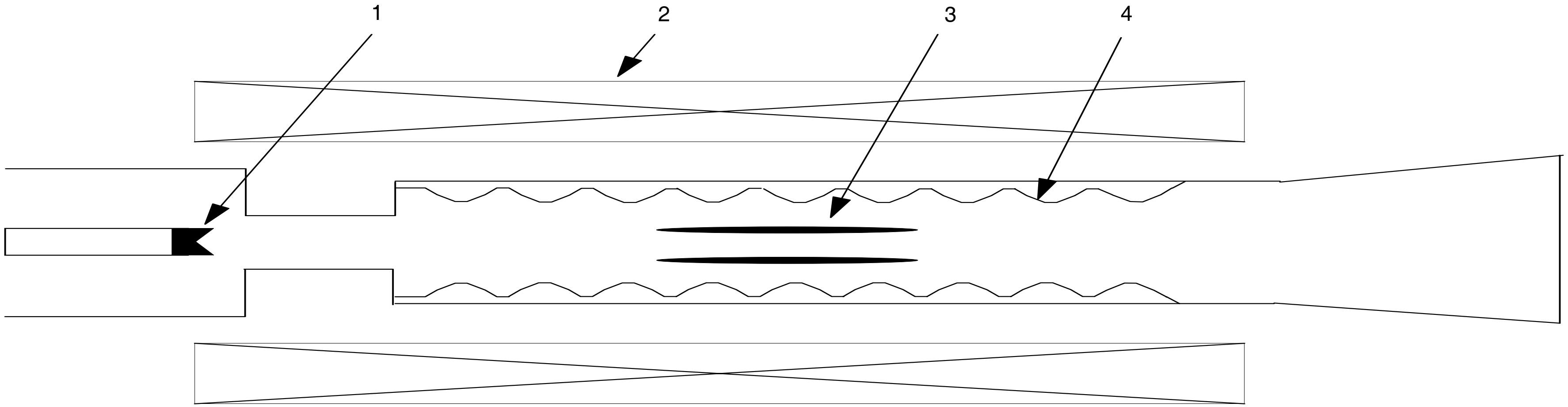

(1) cathode (2) superconducting solenoid

(3) electron bunch (4) slow-wave structure

Compact superradiant source

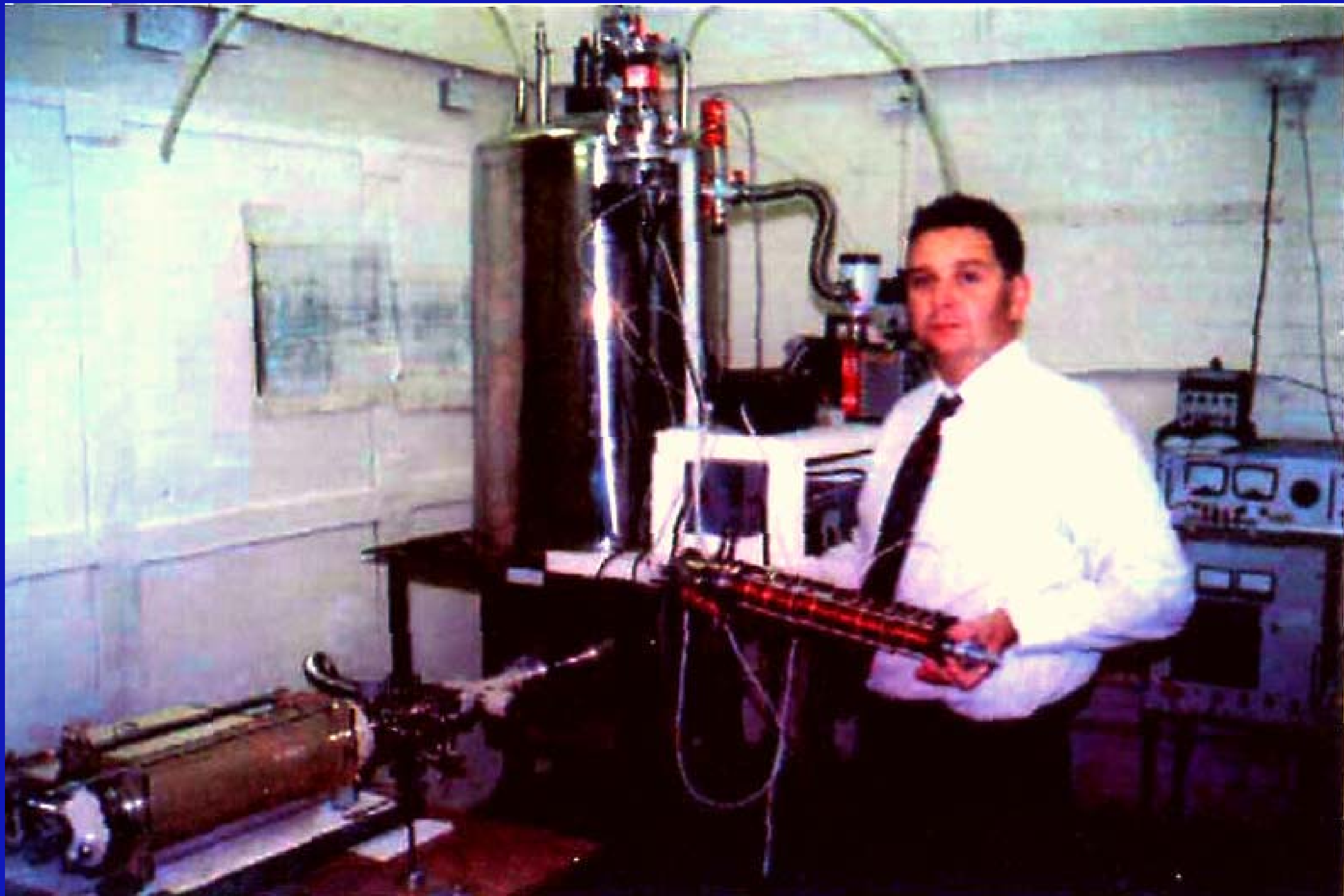

Ginzburg et al, Phelps A.D.R. et al., Shpak V.G. et al.,

1997, Physical. Review Letters, **78**, 2365-2368.

Auroral Kilometric Radiation - AKR

Aurora Borealis – Northern Lights

Horseshoe theory of AKR - Bingham, R. and Cairns, R.A., 2000, Phys. of Plasmas, 7, pp3089-3092

Planetary Magnetospheres

All solar system planets with strong magnetic fields (Jupiter, Saturn, Uranus, Neptune, and Earth) also produce intense radio emission – with frequencies close to the cyclotron frequency.

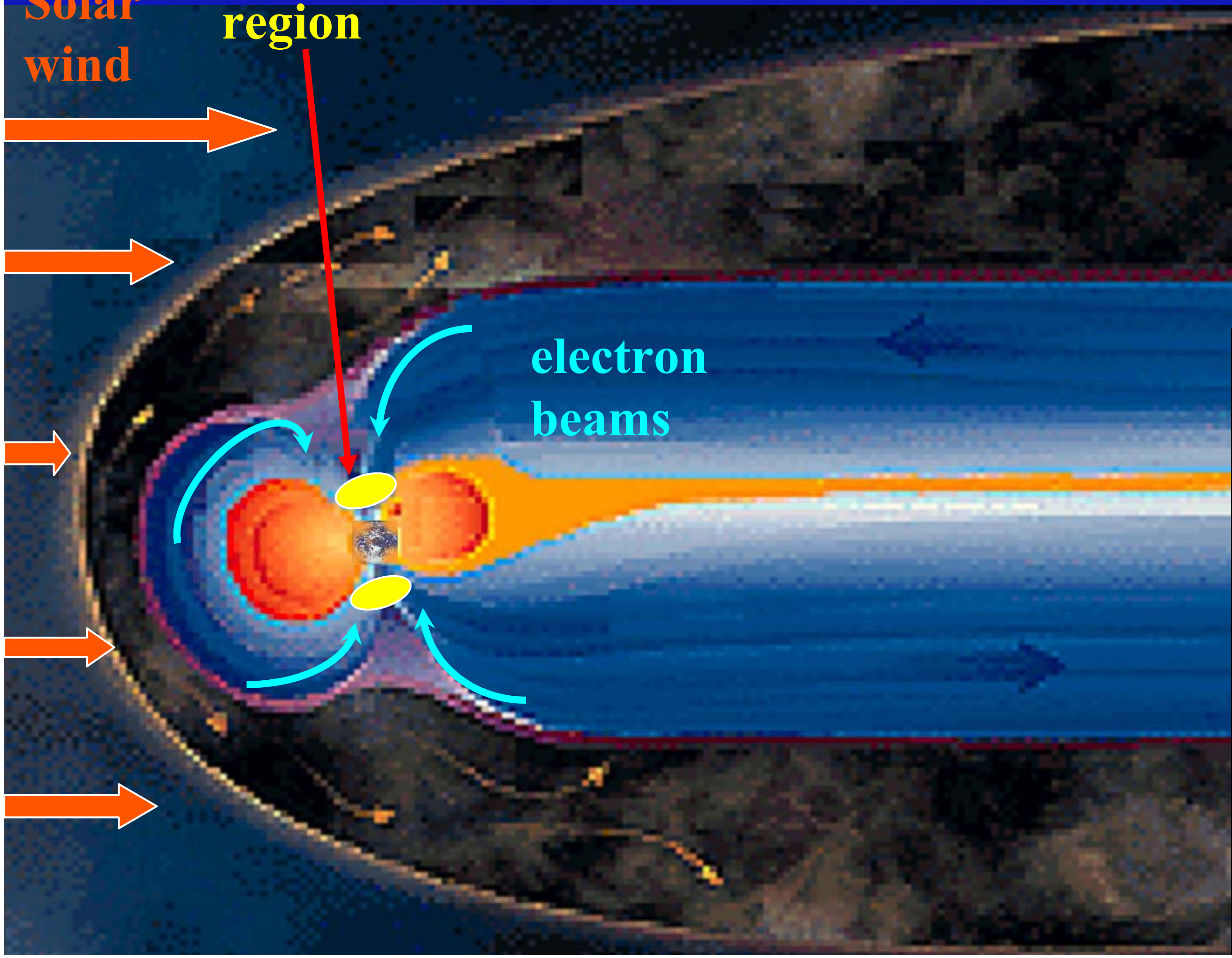

Planetary Aurora

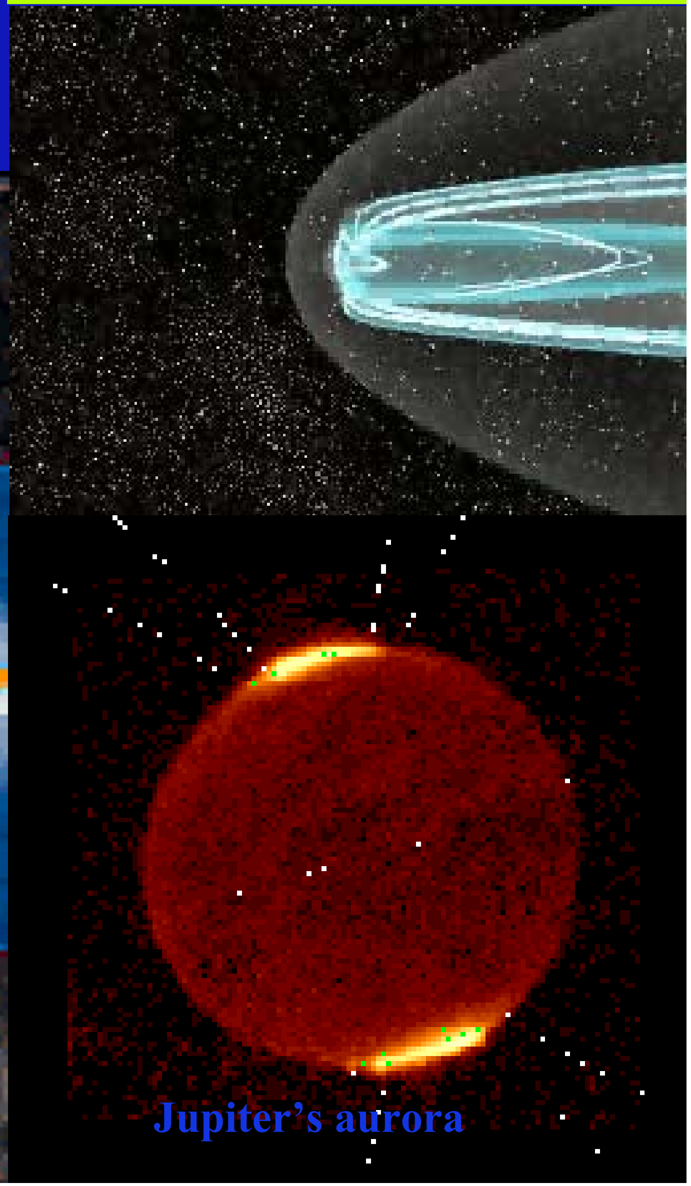

Electron horseshoe distributions in the aurora

DE-1 at 11000 km over the polar cap

Menietti & Burch, JGR, 90, 5345, 1985

FAST Observations Delory *et al.* GRL, 25(12), 2069, 1998

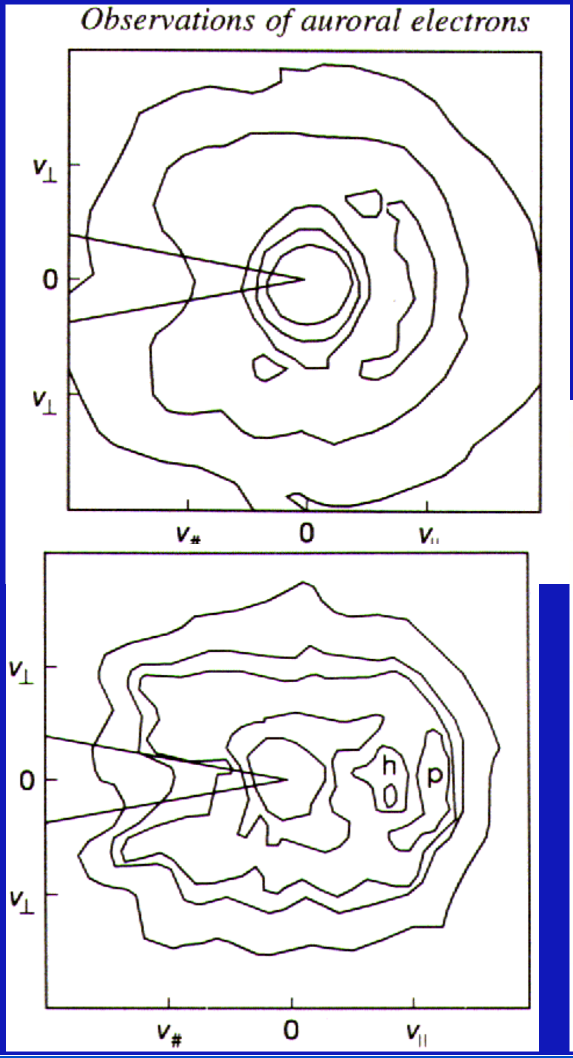

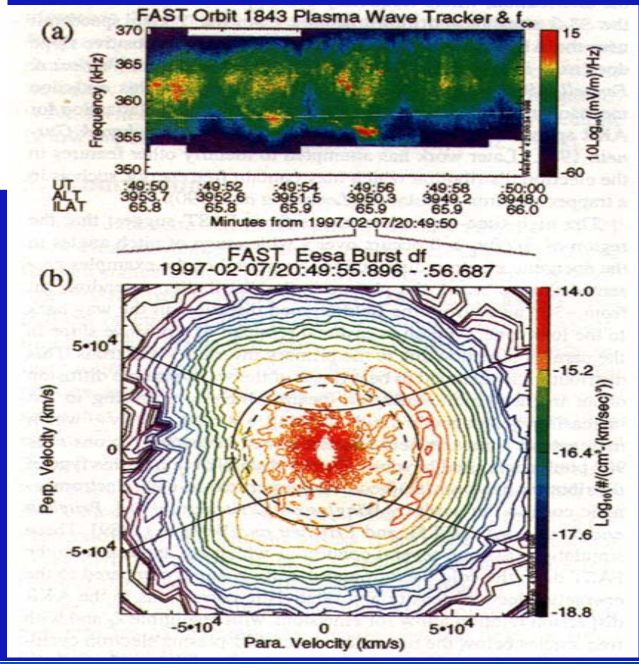

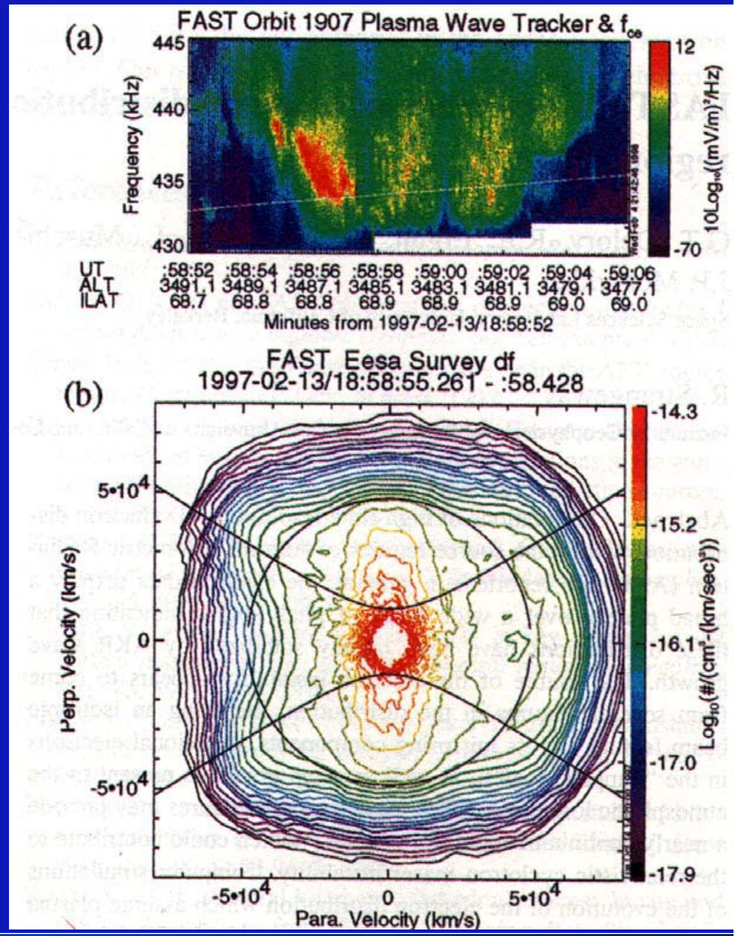

Radiation from horseshoe distribution

Beam moving down converging magnetic field lines. Conservation of magnetic moment means particles lose parallel energy and gain perpendicular energy.

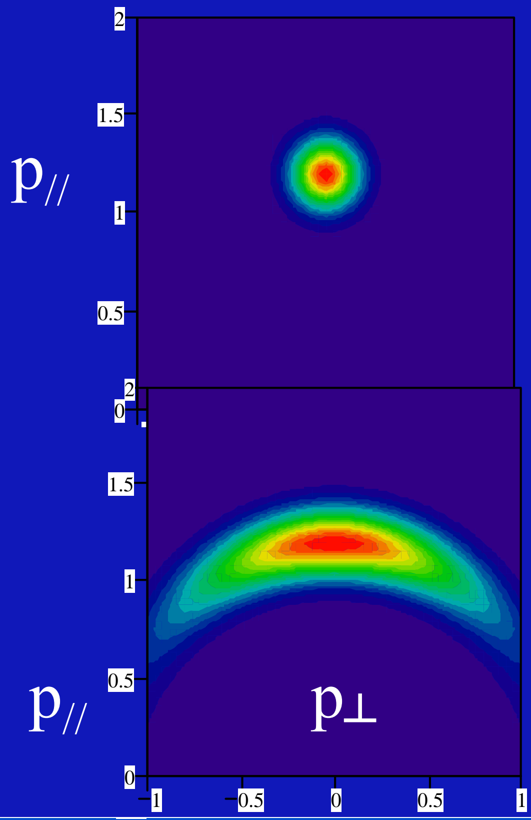

$$\mathrm{Im}(\varepsilon_{xx}) = -\frac{1}{2}\frac{\omega_p^2}{\omega\omega_{ce}}\pi^2\int_{-1}^{1}(1-\mu^2)\,p(1+p^2)\times\left(\frac{\partial f_0}{\partial p}-\frac{\mu}{p}\frac{\partial f_0}{\partial \mu}\right)d\mu$$

A negative imaginary part corresponds to spatial growth of the wave.

- **AKR in the Auroral Zone**
  - Growth rate of a 5 keV electron beam.
  - Cyclotron frequency 440 kHz.
  - Growth distance of order 5 km.

Growth

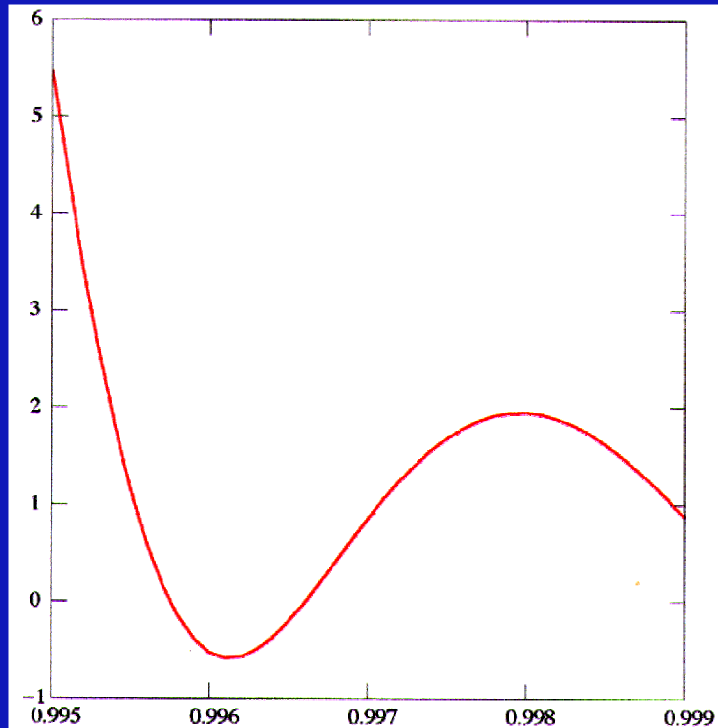

Laboratory simulation of AKR electron flux and magnetic field configuration

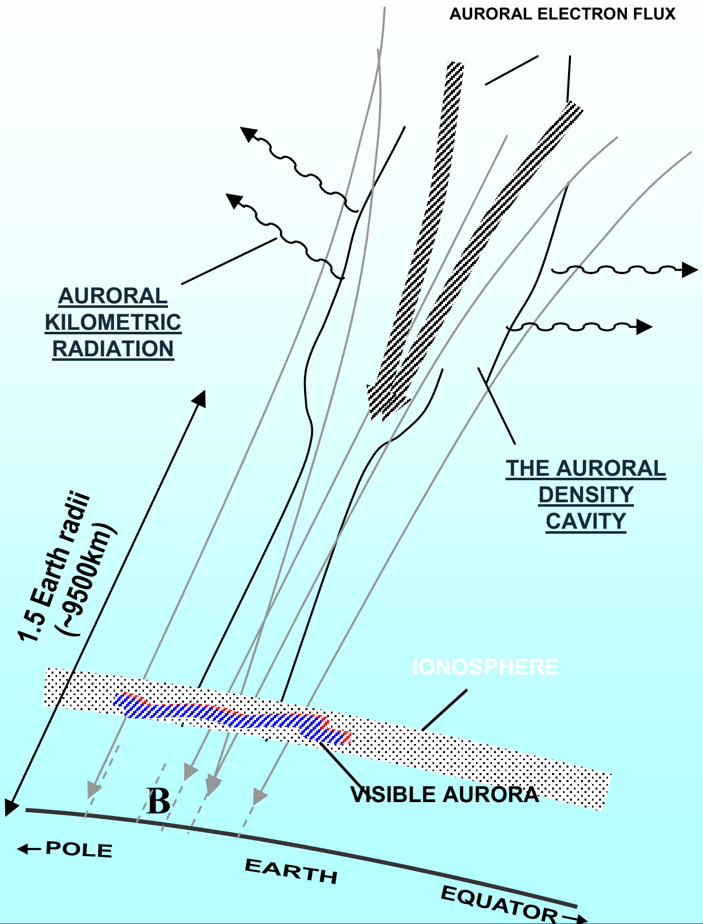

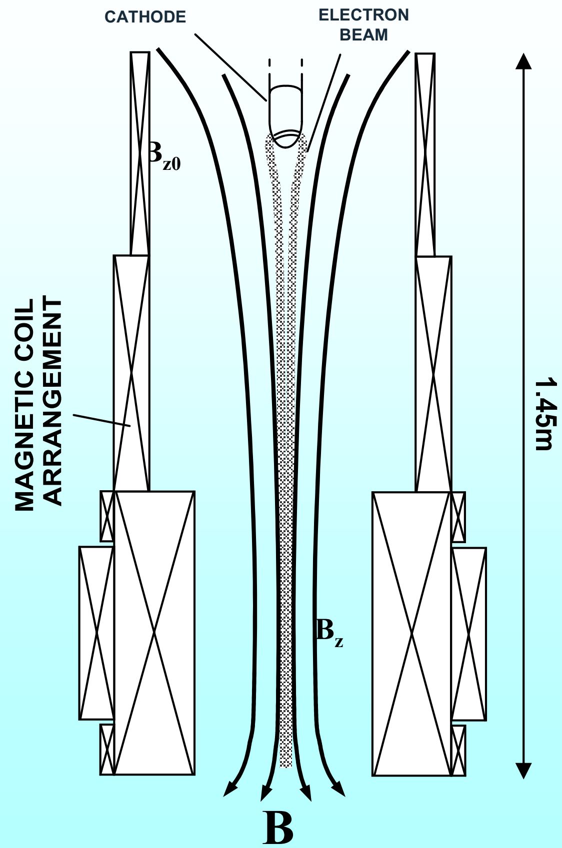

Modelling the space configuration in the laboratory experiment

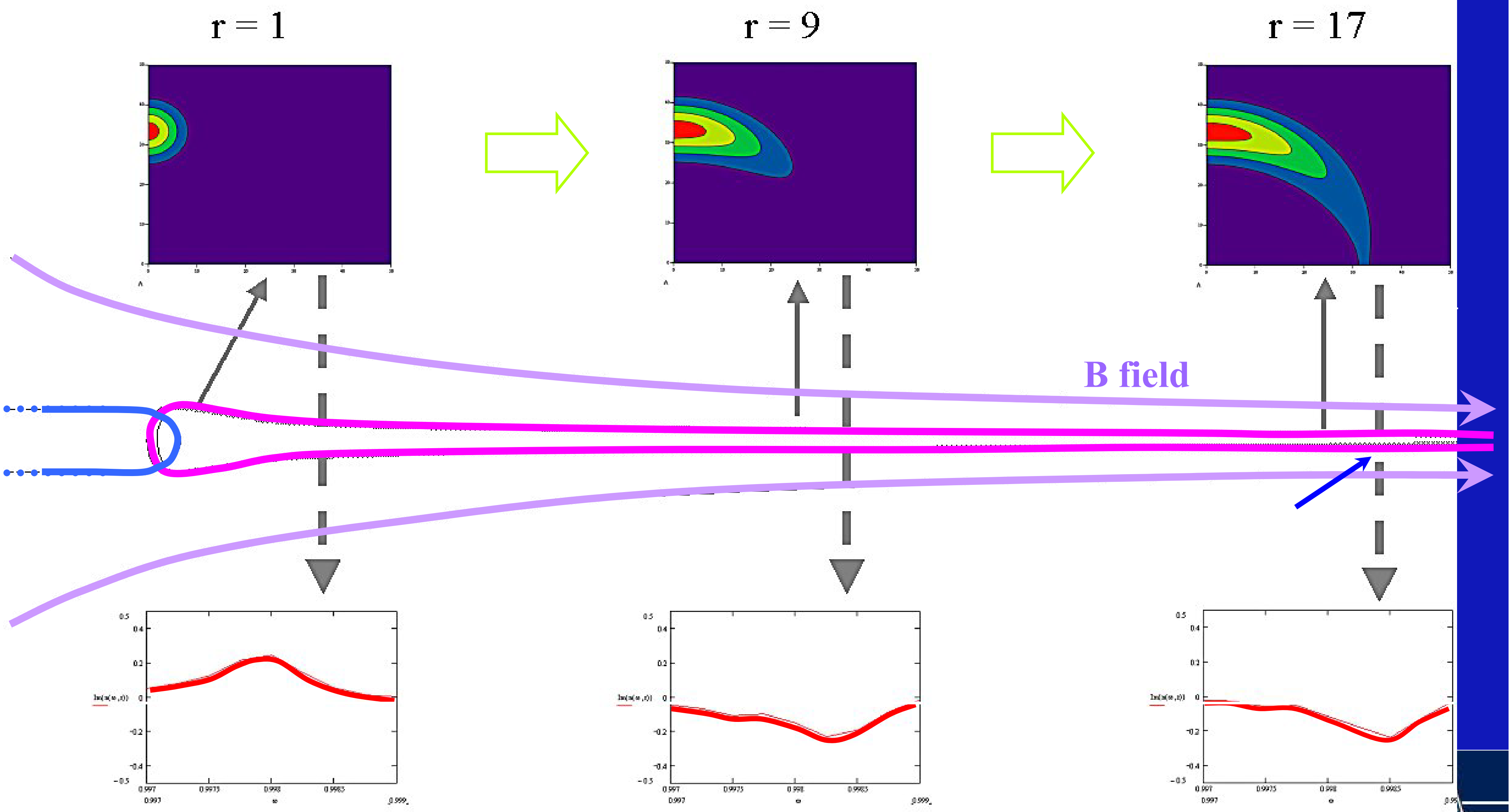

Electron Beam Trajectories Predicted by KARAT

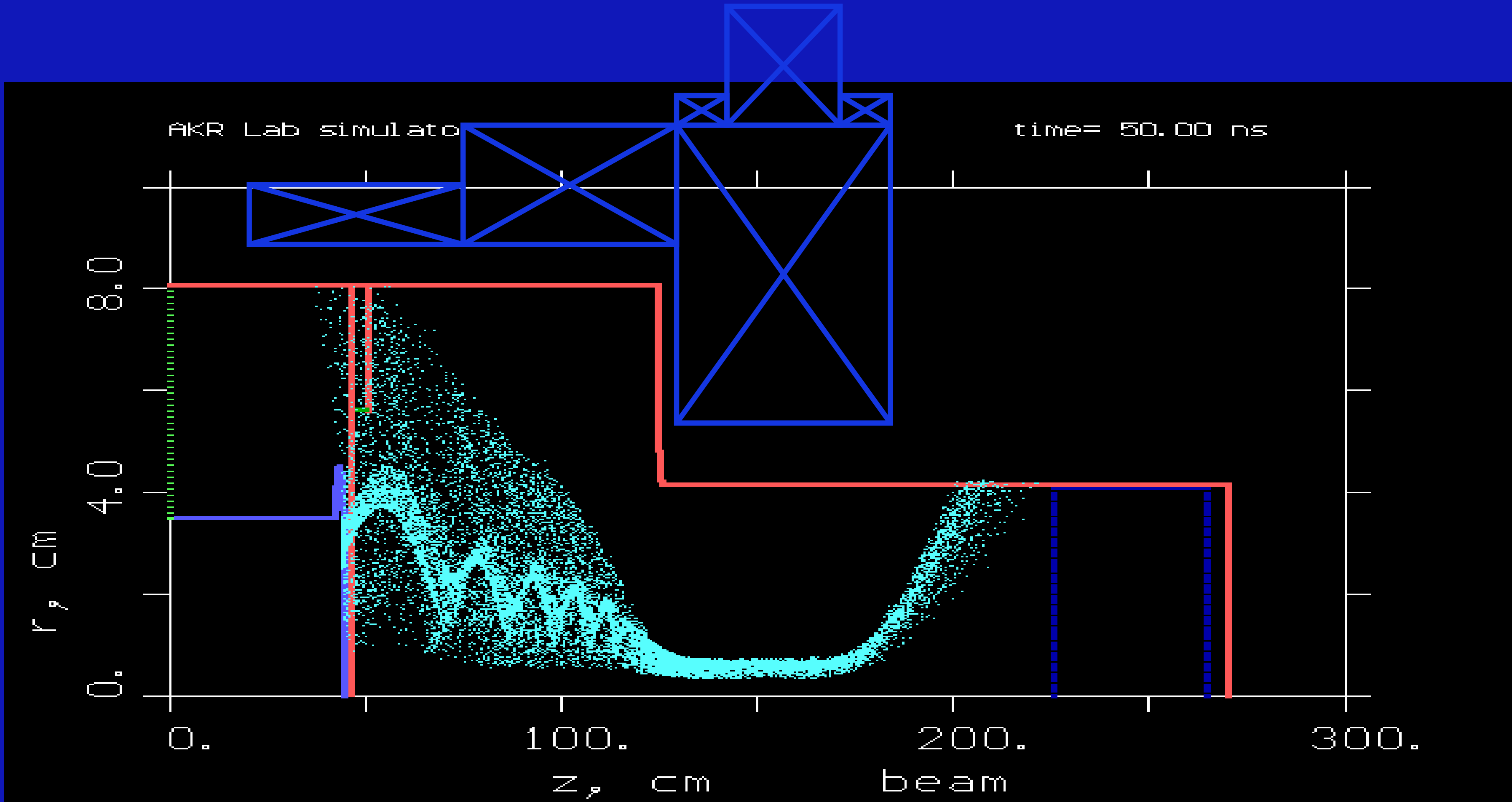

Electron beam trajectory and simulation geometry with solenoids depicted for reference

Phase space results from PiC code KARAT

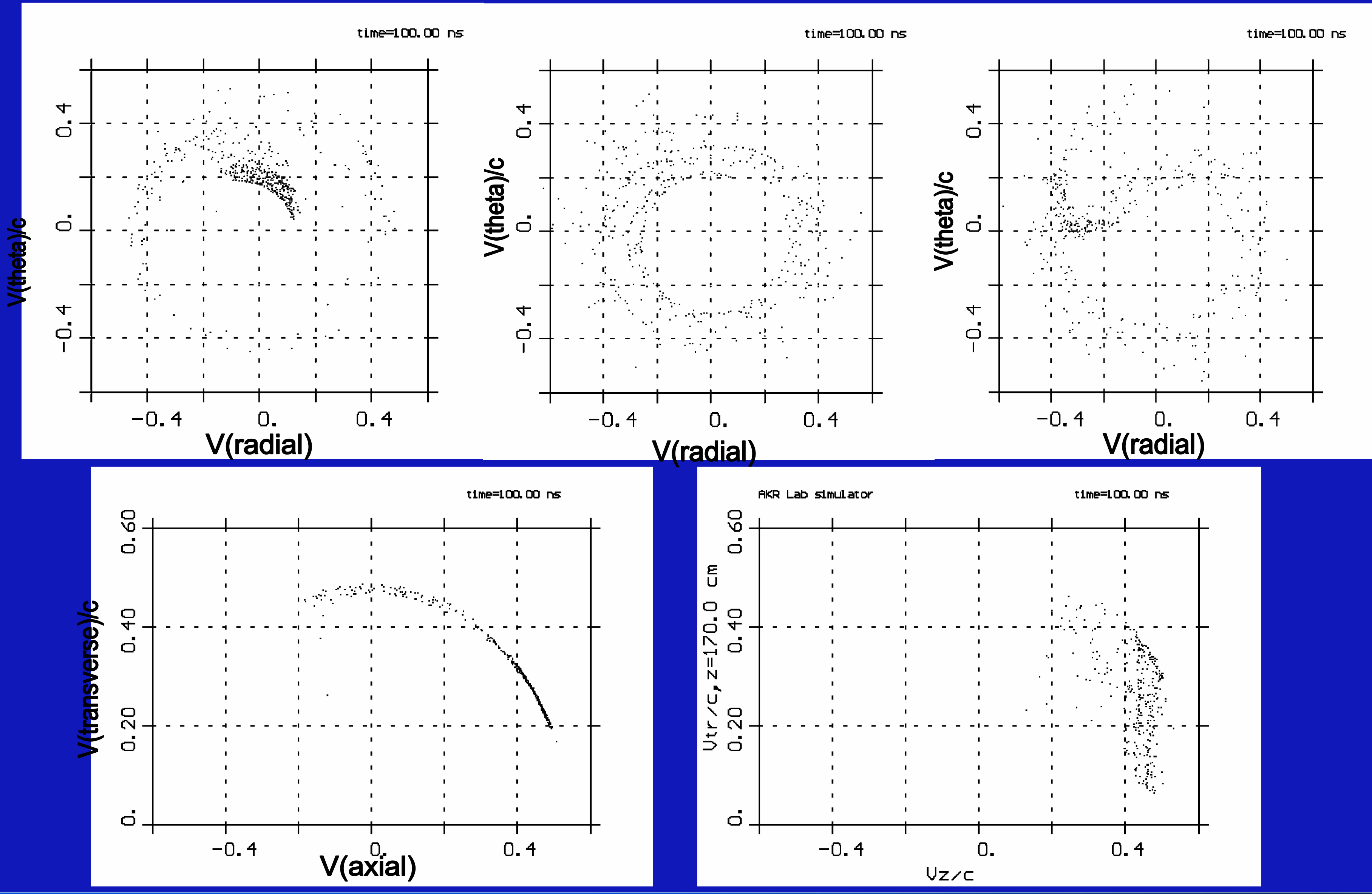

AKR Laboratory Apparatus

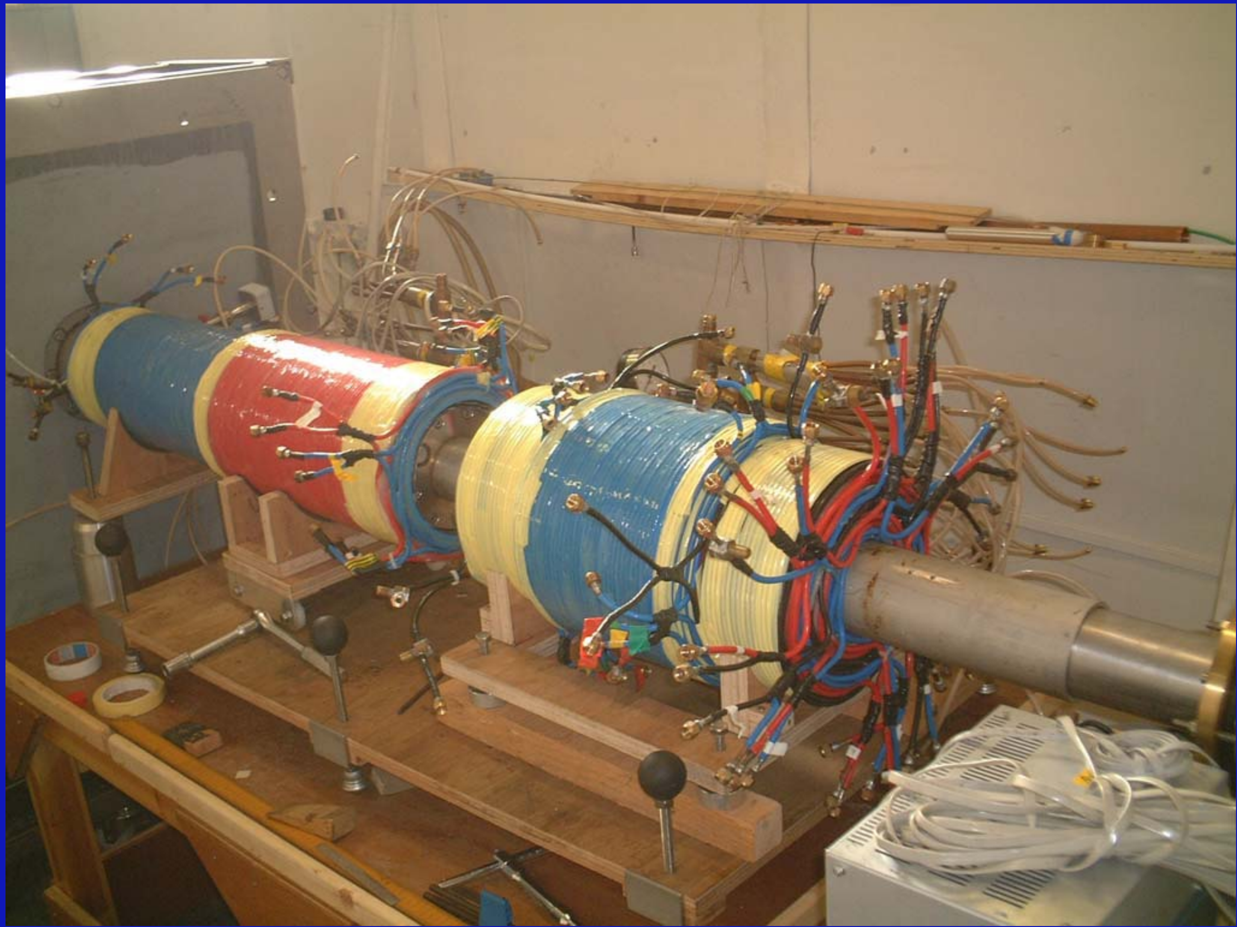

D.C. SPEIRS, I. VORGUL, K. RONALD, R. BINGHAM, R.A. CAIRNS, A.D.R. PHELPS,

B.J. KELLETT, A.W. CROSS, C.G. WHYTE, C. ROBERTSON ,

Journal of Plasma Physics, **71**, 2005, pp 665-674

PiC code simulations for magnetic field of 0.18T

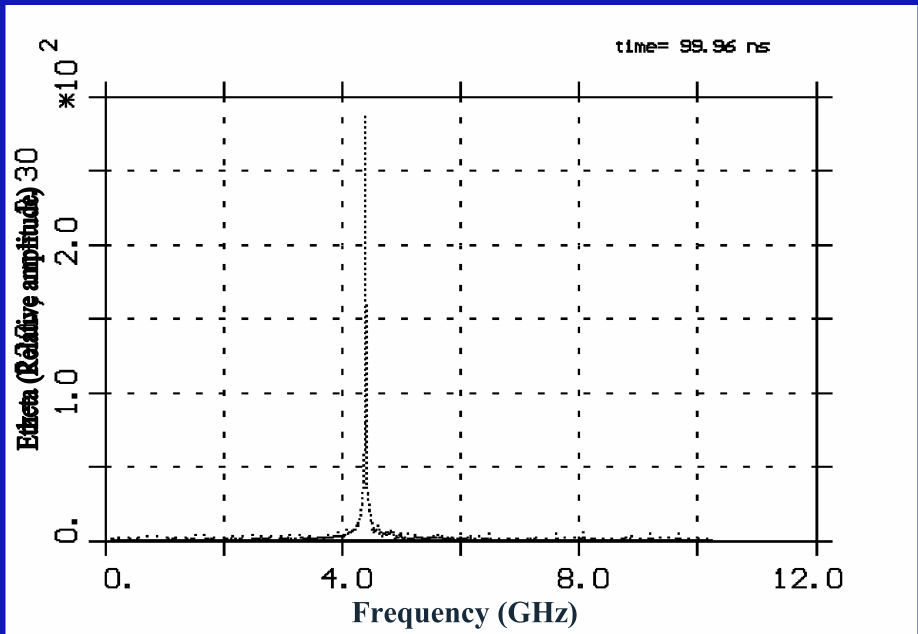

- The KARAT PiC code predicts the output radiation power and frequency
- Best results at 1% cyclotron detuning
- In this case, for 30A on the gun coil, the power was ~20 kW, η=1.8%
- 60A gave ~1 kW, η=0.07%
- The operating frequency predicted by the simulations ~4.45GHz, agrees with our theoretically expected value

Experimental results at magnetic field of 0.18T

Fourier transform showing a peak signal at ~4.45GHz, i.e. close to our cut-off for TE_{01}, best results at cyclotron detuning ~2.4%

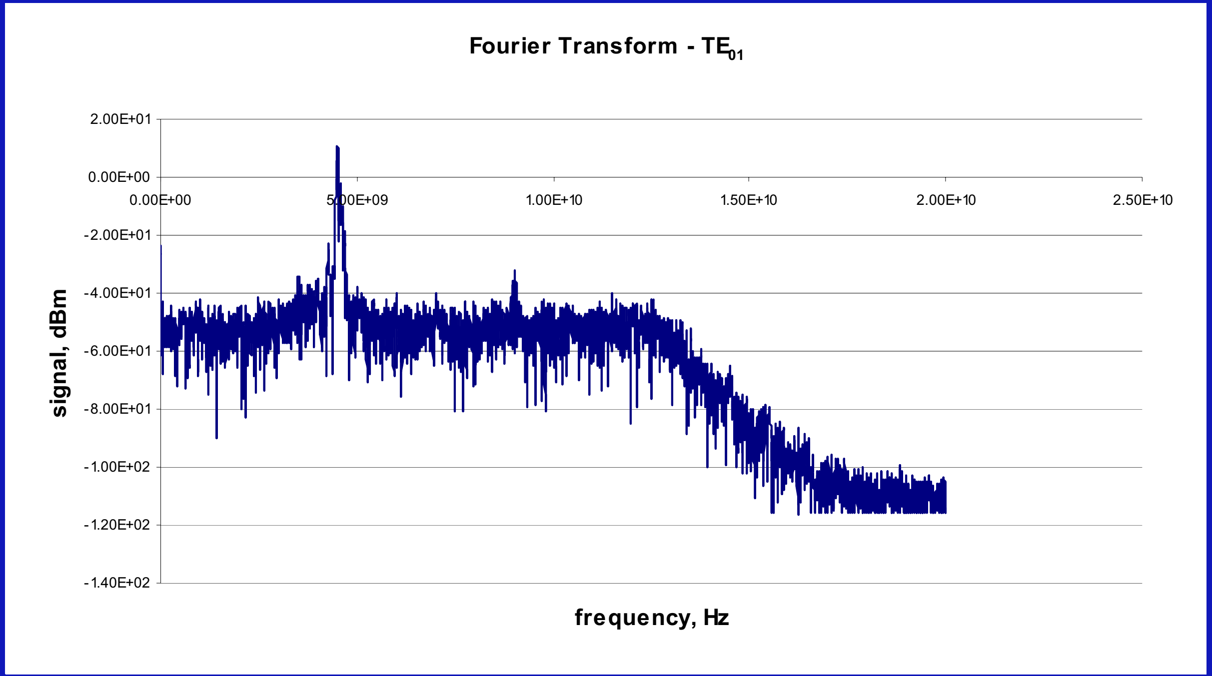

Conclusions

- Eelectromagnetic wave generation by relativistic electrons is a subject that is important in both laboratory and space plasma physics

- Experimental measurements consistently agree with the theory and simulations

- The field has an exciting future as there are many problems still to be solved and applications waiting to be exploited